#5354

SCALE MODELS AND CFD FOR THE ANALYSIS OF AIR FLOW IN PASSIVELY VENTILATED BUILDINGS

G.S. Barozzi[ε], M.S. Imbabi[*], E. Nobile[ε] and A.C.M. Sousa[†]
[ε]Istituto di Fisica Tecnica, Universita degli Studi di Trieste, 34127 Trieste, Italy
[*]Department of Engineering, King's College, University of Aberdeen, Aberdeen AB9 2UE, United Kingdom
[†]Department of Mechanical Engineering, University of New Brunswick, Fredericton, N.B., Canada E3B 5A3

ABSTRACT

A new bioclimatic building concept based on solar-driven ventilation is analysed through the use of physical and numerical modelling. Measurements are conducted for a 1/12th laboratory scale model designed to replicate the full-scale prototype and its micro-climate. Predictions are obtained by employing advanced Computational Fluid Dynamics (CFD) techniques, and the experimental results provide the benchmarking required in the development of the numerical model, which may offer a viable alternative to expensive and hard to set full-scale tests. The combination of laboratory and computational results gives additional physical insight into the prevailing phenomena determining the ventilation levels, and a first assessment on the feasibility of the concept.

Comparison between predictions and experiments indicates a very favourable agreement.

INTRODUCTION

Developing nations face the unique challenge of raising the living standards of their ever-growing populations, while their economies carry huge debts and are limited by finite, often shrinking, resources. Many factors can be singled out as prime candidates to this unfortunate situation, but no minor role can be attributed to imported technologies that have ignored and/or are very foreign to the local existing conditions. In particular, when dealing with building design, imported technologies in many cases have had disastrous results, not only in terms of high capital, operating and maintenance costs, but by leading to the destruction of traditional socio-economic structures. To avoid the repetition of past errors, there is a clear need to further R&D in building design that is best suited to severe climates and, concurrently has low capital and operating/maintenance needs and is environment-friendly. The task, no doubt, is formidable in view of the multi-objective characteristics of such a design and its obvious budgetary constraints.

In the present work, the priority target is addressed to energy efficiency and associated analysis. This choice is not surprising, when best estimates indicate that in today's world 30 to 50% of the total energy consumption is spent in establishing appropriate thermal comfort levels in buildings.

The bioclimatic building concept to be analysed in the present study features an integrated solar chimney roof to promote free convection-driven ventilation. Recently, a prototype of this building was constructed in Nigeria (Costa et al. 1986), as part of a field experiment in passive solar architecture. A solar chimney roof was selected to allow hot air to rise and exit through the apex, drawing cool outdoor air through the interior of the building in a continuous process. Unfortunately, the design was conducted with no rigorous method of analysis, and the prototype was not instrumented to provide a full assessment of the concept (Piva 1989). In this study an attempt is made in order to obtain a better physical insight into the phenomena, which are relevant in yielding adequate ventilation levels. The system, despite its conceptual simplicity, poses serious questions regarding effectiveness, and ultimately feasibility. CFD, as outlined by many authors (e.g., Clarke 1987), is an ideal tool to test and evaluate new building designs and strategies. This analysis approach will be employed in the present work, and will be benchmarked by experimental data gathered for a 1/12th scale model.

SMALL SCALE MODEL

Background

The full scale prototype was built in Ife (Nigeria), latitude of 7.5°N and longitude of 4.6°E, as part of a collaborative research program between the Building Laboratory of Obafemi Awolowo University (Nigeria) and the Istituto di Architetture e Urbanistica of the University of Trieste (Italy). The prototype consists of a 5.5 x 3.5 x 3.0 m^3 single room, with a corrugated metal roof and fibre-board ceiling. Details on the materials used and construction procedure are given in (Costa et al. 1987).

The model was built on a 1/12th scale of the prototype, and particular efforts were made to guarantee that every geometric detail was fully represented. Also, when viable, the thermophysical properties of the materials of construction for the model and prototype were similar. Selection of the dimensions, materials of construction, and operating parameters for the model was conducted through an extensive parametric analysis (Imbabi and Chiesa 1990).

The external environment was considered to be defined by the ambient temperature (T_0), external air velocity (W_0), and global (G_s) and diffuse (D_s) solar radiation. Since de-humidification is expected to be minor, the influence of relative humidity is disregarded in the model. The temperature of the air surrounding the test chamber was assumed to represent T_0 for the model. Measurements were made for quiescent conditions, $W_0 = 0$; since, as expected, these conditions will place the highest demand upon the solar-assisted ventilation. The relevant dimensions and constructive details of the model are given in Figure 1.

A four-lamp 30 cm centre-to-centre rectangular array was used to reproduce the solar irradiation in the small-scale model. The lamps are manufactured by Osram and sold under the trade name ULTRA-VITALUX. Each lamp is rated at a power of 300 W and the array produces approximately 1000 W/m^2 when normal to a plane 50 cm distant, and for simplicity and to remove time-dependent

conditions, the array was maintained at a fixed position directly above the model's roof. This arrangement will ensure maximum roof exposure, and in the absence of wind (W_0 = 0), will represent the conditions for which ventilation will be most needed.

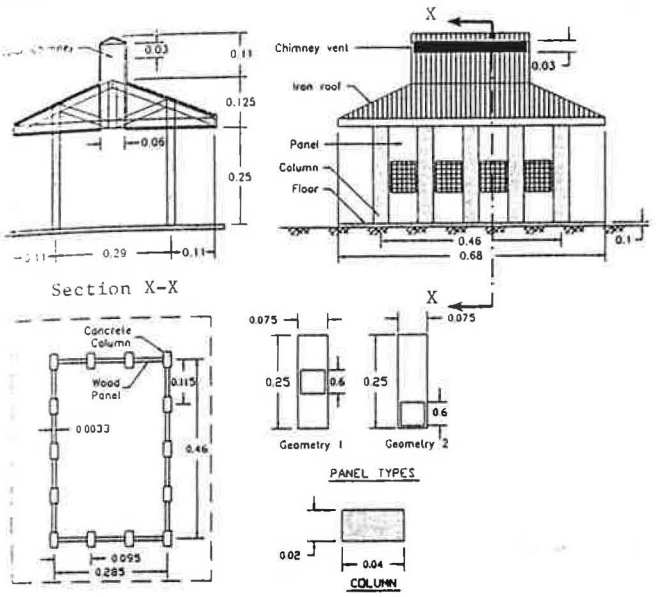

Figure 1. Details and dimensions (m) of the 1/12th scale model.

Experimental Procedure

An IBM AT - compatible microcomputer, fitted with a Burr-Brown DMA series 20000 carrier, and 12 bit A/D plus 16 bit D/A converters, was used for data acquisition. Twelve input channels were used for temperature measurement performed by miniature platinum resistance thermo-detectors. Input data from these channels was sampled 18000 times every 10 seconds, and averaged to give an overall accuracy of ±0.2 K, and automatically stored in a data file.

A DANTEC 54N50 low velocity anemometer was employed for the air velocity measurements, which are performed at a number of sections across the model. It is estimated that in regions of low velocity, despite all precautions taken, the measurements may have an accuracy no better than ±20%. Steady-state conditions were reached approximately one hour after the lamp array is switched on, and by then, the values measured are written to an output file. Temperatures and velocities were measured at several sections across the width of the model as defined by a reference vertical plane, X-X (Figure 1); in addition, temperatures are taken at six points on the metal roof. To achieve the dual goal of zero-external air flow, and maximum accuracy and repeatibility of the measurements every effort was spent to minimize possible disturbances that may affect the experimental conditions such as air movement caused by external drafts and personnel traffic, and vibrations exerted upon the test chamber.

NUMERICAL SIMULATION

Introduction

Over recent years there has been an increasing awareness of the potential that CFD offers in the analysis of building related issues, with particular emphasis on applications dealing with energy and safety. The literature in the field has been growing at a steadily pace, and among others relevant technical papers to the present study are (Nielsen, Restivo and Whitelaw 1979; Mirakami and Kato 1989; Awbi 1989; Davidson 1989). This investigation, however, differs from most of the reported work in the sense that the system under investigation performs under the thermosyphon principle. Modelling of this problem poses some difficulties, particularly in what concerns the setting of the boundary conditions, and as will be discussed, there are some uncertainties associated with these. Considering the exploratory nature of this investigation, a few simplifications were introduced, of which the most important is the two-dimensionality assumption. In this regard, the 2D region of study corresponds to a 2D transversal section across one of the windows. Additional assumptions are as follows:

- Flow and thermal fields are steady and laminar;
- Radiation and conjugate heat transfer effects are negligible.

The rationale for these assumptions is to a great extent based on computational expediency, however, a few physical considerations should be advanced. The assumption of steadiness is directly related with the conditions selected for the experiments. It should be noted, however, that in the full-scale prototype, the fluid flow and heat transfer will be most likely subject to a certain level of unsteadiness, not only due to the variability of the atmospheric conditions but also due to the movement of the occupants of the building. The inclusion of conjugate effects in the model is not justifiable in this study, since they are not expected to affect the heat transfer by more than 1 to 3%. Moreover, radiation, considering the low temperatures that this investigation deals with, is negligible as compared to the overall heat transfer, although it may be influential in determining thermal comfort levels for the occupants, a particular aspect, which is beyond the immediate concern of the present study.

With the objective of removing further uncertainties in the simulation, the actual experimental temperatures are used as boundary conditions at the model's roof. By following this path, the modelling of the radiative load is not required.

Governing Equations

The two-dimensional, steady-state, laminar fluid flow and energy equations are coupled through the buoyancy term, and the Boussinesq approximation is employed. The length scale selected is the height, H, of the experimental model, and the reference temperature is T_0. The temperature, T_1, the highest measured temperature at the metal roof, is also employed in the normalization of the temperatures.

The normalized variables are defined as follows:

$$x = \frac{X}{H} \; ; \quad y = \frac{Y}{H} \; ; \quad u = \frac{UH}{\alpha} \qquad v = \frac{VH}{\alpha} \; ; \quad p = \frac{PH^2}{\rho\alpha v} \; ; \quad t = \frac{T - T_0}{T_1 - T_0} \qquad (1)$$

The normalized equations in Cartesian coordinates governing mass conservation, momentum and energy are given as:

$$\frac{\partial u}{\partial x} + \frac{\partial v}{\partial y} = 0 \qquad (2)$$

$$\frac{1}{Pr}\left(u\frac{\partial u}{\partial x}+v\frac{\partial u}{\partial y}\right)=-\frac{\partial p}{\partial x}+\left[\frac{\partial^2 u}{\partial x^2}+\frac{\partial^2 u}{\partial y^2}\right] \quad (3)$$

$$\frac{1}{Pr}\left(u\frac{\partial v}{\partial x}+v\frac{\partial v}{\partial y}\right)=-\frac{\partial p}{\partial y}+\left[\frac{\partial^2 v}{\partial x^2}+\frac{\partial^2 v}{\partial y^2}\right]+Ra\cdot t \quad (4)$$

$$u\frac{\partial t}{\partial x}+v\frac{\partial t}{\partial y}=\left[\frac{\partial^2 t}{\partial x^2}+\frac{\partial^2 t}{\partial y^2}\right] \quad (5)$$

The dimensionless parameters, Pr (Prandtl number) and Ra (Rayleigh number) are defined as

$$Pr=\frac{\nu}{\alpha} \quad (6)$$

$$Ra=Pr\times Gr \quad (7)$$

where Gr denotes the Grashof number, which is defined as

$$Gr=\frac{\beta g H^3 (T_1-T_0)}{\nu^2} \quad (8)$$

Since, the boundary conditions for the numerical model are symmetric, and since the numerical simulation is for steady-state, only the half-section needs to be modelled, as shown in Figure 2.

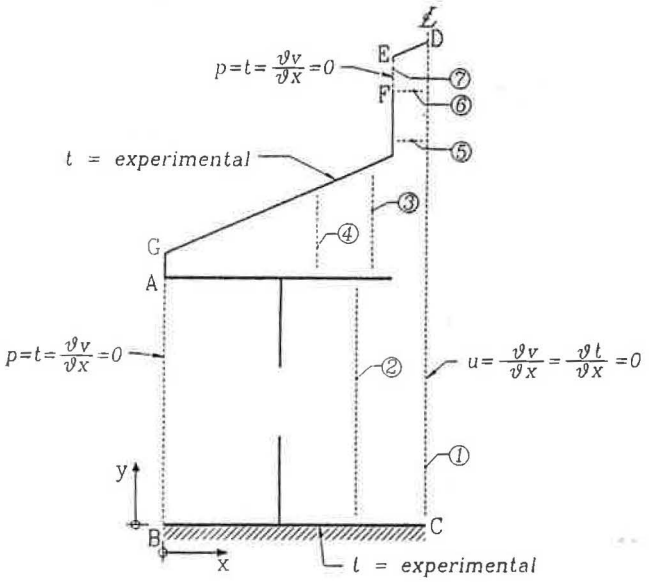

Figure 2. Computational domain and boundary conditions.

The boundary conditions used, as referred to Figure 2, are:

1. Velocity.

$$\begin{array}{llll} A-B: & \frac{\partial v}{\partial x}=0 & B-C: & u=v=0 \\ C-D: & u=0; & D-E: & u=v=0 \\ E-F: & \frac{\partial v}{\partial x}=0 & F-G,\ G-A: & u=v=0 \end{array} \quad (9)$$

The velocity components are also set to zero at all internal walls.

2. Pressure. The values of pressure are specified at inlets and outlets as follows:

$$A-B:\ p=0 \qquad E-F:\ p=0 \quad (10)$$

3. Temperature.

$$\begin{array}{llll} A-B: & t=0 & B-C: & \frac{\partial t}{\partial y}=0 \\ C-D: & \frac{\partial t}{\partial x}=0 & D-E: & t=1 \\ E-F: & t=0 & F-G: & t=t_{experimental} \\ G-A: & \frac{\partial t}{\partial x}=0 & & \end{array} \quad (11)$$

The choice of boundary conditions, as stated before, required careful decisions. For instance, the setting of the boundary condition A-B requires some experimentation, since its location should be such that it causes no disturbance to the flow crossing the aperture.

Based on previous work reported in the literature (Markatos, Malin and Cox 1982; Schreuder and Du Plessis 1989), two simplifying assumptions were introduced into the boundary conditions, namely:

- Pressure recovery is neglected for the outflow (E-F), i.e., the jet is assumed to be purely buoyant.
- The kinetic head is not considered at the inlet boundary A-B.

SOLUTION ALGORITHM

The full description of the numerical technique is fully reported elsewhere (Nobile, Russo and Barozzi 1989). Here, for the sake of brevity, only the main features will be outlined.

The method used to solve Eqs. 2. to 4., as well as the energy conservation equation, Eq. 5., is based on a control volume segregated procedure. The solution domain is subdivided into small sub-domains (control volumes or finite volumes) by a variable size rectangular grid. A staggered grid is used, on which all scalar quantities are located at the center of the finite volumes, while the velocity components are located at the volume faces.

For the general conserved variable, ϕ, the discretized conservation equation at a point P is written in the form

$$a_P\phi_P=a_N\phi_N+a_S\phi_S+a_E\phi_E+a_W\phi_W+b \quad (12)$$

where a_P, a_N, a_S, a_E, a_W are the linearized coefficients of the equation and $\underline{b}$ is a source term.

Since the governing equations are coupled together and are highly non-linear, an iterative approach based on a segregated algorithm (Van Doormaal and Raithby 1984) with an enhanced solver (Theodossiou and Sousa 1986) is used for their solution, whereby a cyclic outer iteration is employed comprising the following sequence of operations:

1. The momentum equations, Eqs. 3. and 4., in a discretized form similar to Eq. 12., are solved

based on a best estimate for the pressure field taken from the previous iteration.

2. A Poisson-type equation for the pressure correction, derived from the continuity equation, Eq. 2., is solved, and at the end of each outer iteration loop, pressure and velocities are corrected.

3. The energy equation, Eq. 5., in discretized form, is then solved.

4. A new cycle is commenced unless the solution is judged to be converged. This is the case when the normalized Euclidean norm of the values of the residuals over the field for each variable falls below a specified small value. The value used in this study is 10^{-6}.

The computation was performed on 56 x 96 non-uniform, Cartesian grid, with appropriate stretching close to the walls in order to capture the thin boundary layers which arise at high Rayleigh numbers. Guidance for the grid-convergence tests is primarily obtained from work performed by the present authors (Nobile, Sousa and Barozzi 1990). About 2000 iterations were required to satisfy the above specified convergence criteria.

RESULTS AND DISCUSSION

The experimental data for the temperature at the model's roof are obtained at six different locations as shown in Figure 3. The measurements indicate that for the thermal load employed the value of the maximum averaged temperature, T_1, is 44.5°C. The ambient temperature, T_0, was maintained at a uniform and constant value of 23.8°C.

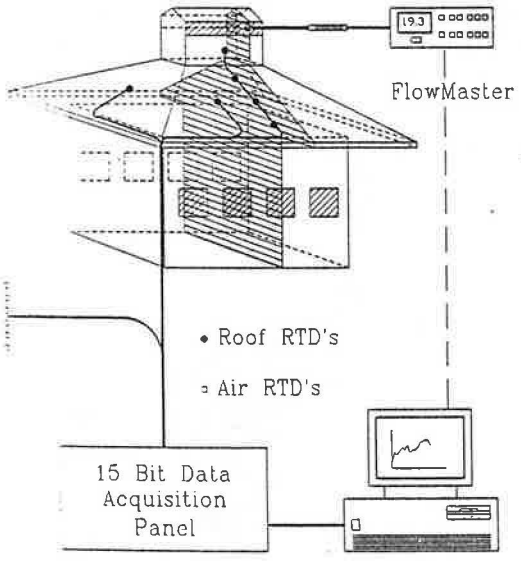

Figure 3. Data acquisition system and location of temperature sensors. Dashed area denotes 2-D computational domain.

The Rayleigh number based on the above-mentioned experimental conditions is 1.9×10^8, which establishes that the core flow should be in the laminar regime, and its main trends should be adequately described by the model selected. The Prandtl and Rayleigh number values of 0.71 and 1.9×10^8, respectively, were used in all computational runs reported in this study.

In Figure 4 the computational velocity streaklines depict very clearly the flow pattern, which to some extent, has a few surprising features. The incoming flow shows close resemblance to a bent, high-momentum, free jet, with little diffusion being observed. This leads, except for the ventilation "corridor" to large regions of quiescent air, with obvious detrimental effects upon adequate comfort levels. The simulation predictions of the location and intensity of the recirculating eddy occurring above the ceiling partition are in remarkable agreement with the observations conducted by using a whole-field visualization technique (Barozzi et al. 1991). The procedure consists of generating quasi-buoyancy neutral smoke and then by a laser sheet the smoke traces are visually enhanced.

Along the inclined inside roof surface, the horizontal structural beams have a considerable effect upon the flow. Wakes and recirculations are generated in patterns similar to flow over bluff bodies. These flow features increase the mixing levels, yielding higher heat transfer rates as observed in ribbed surfaces (Ciofallo and Collins 1989). The computations clearly indicate highly non-symmetric velocity profiles along the height of the chimney. The bulk of the flow is confined to about 60% of the cross-section of the chimney, a feature already noted for confined convective flows (Nobile, Sousa and Barozzi 1989).

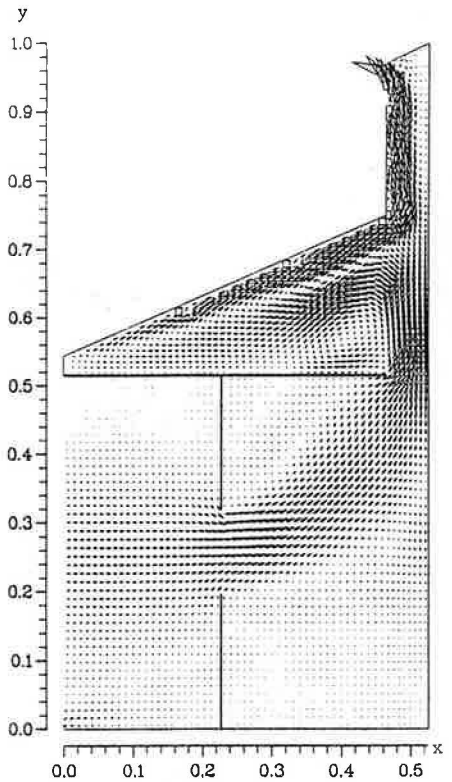

Figure 4. Computational velocity streaklines.

Figure 5 further illustrates the main features of the flow field by employing a shadowgraph representation. It should be reiterated that in most of the living area of the room the velocities are well below 0.01 m/s, which may yield less than appropriate ventilation levels.

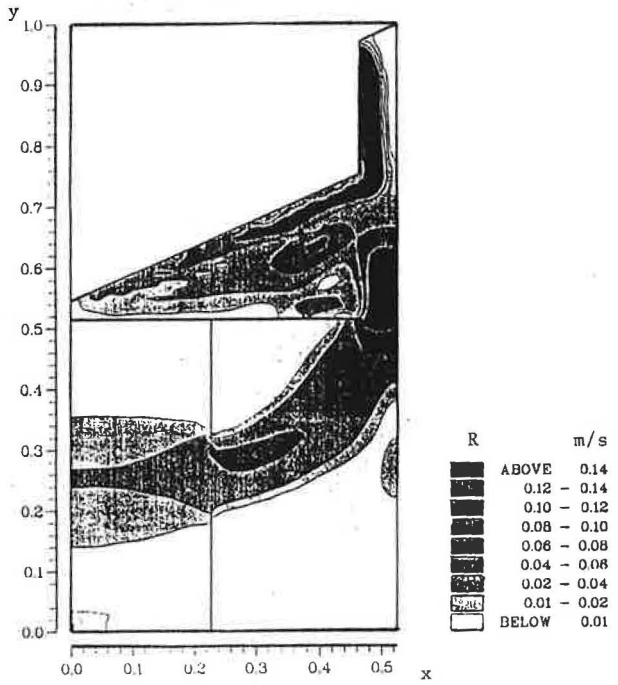

Figure 5. Shadowgraph representation of velocity field. [$R = (V^2 + U^2)^{1/2}$]

The temperature field is mapped in Figure 6; strong thermal stratification can be clearly identified in the under-roof region. Its occurrence is physically realistic, and is in agreement with the flow patterns analysed in Figures 4 and 5. Heat conduction across the partition wall is fully taken into account in the simulation, and this explains the "pocket" of hot air located under the partition as depicted in Figure 6.

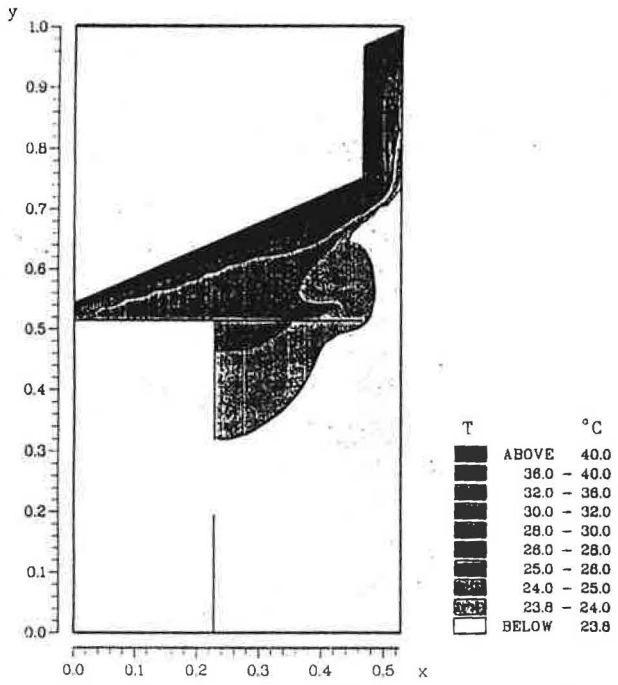

Figure 6. Map of the computed temperature field.

Measurements were performed in seven different sections of the physical model, this location is indicated in Figure 2, and each section is identified by a number. Since space precludes it, only a few representative comparisons between predictions and experiments will be reported here.

As discussed earlier on, the modelling of the inlet and outlet boundary conditions, with particular relevance to the latter one, is of some concern. Predictions and experimental data for the outflow velocities at section #7 are presented in Figure 7. The agreement between the predicted and measured trends is highly encouraging, for instance the location of the maximum velocity is predicted within an accuracy of less than 0.1%. The discrepancy between the magnitude of the predicted and measured velocities, however, still needs to be elucidated. One plausible explanation may be related with the use in the simulation of a mean value for the viscosity, while at the outlet, the viscosity reaches its minimum value. This is consistent with the lower magnitude of the computed velocities as compared to the experimental values.

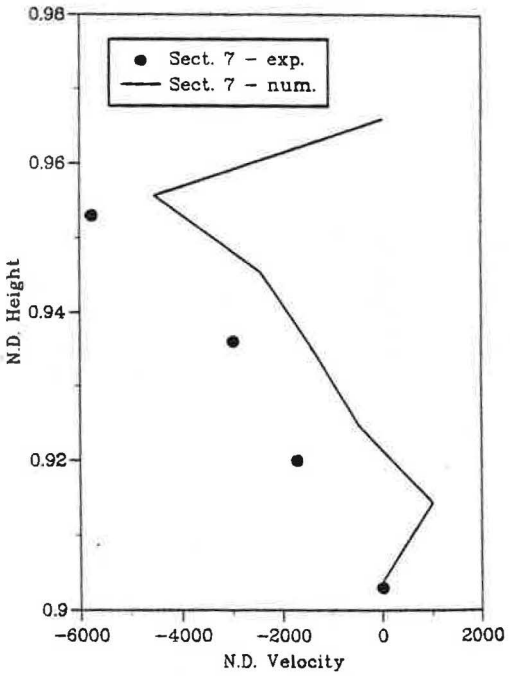

Figure 7. Predictions and experimental data for the velocities at the outlet section (Section #7).

Figure 8 (a) and (b) depicts comparisons between the measured and predicted temperature profiles for sections #1 and #2, respectively. Their overall agreement is good, and some of the differences may be attributed to the choice of reference values and boundary conditions at the roof surface. Moreover, the techniques for the measurement of velocity and temperature being themselves intrusive, may cause serious disturbances upon the velocity and temperature fields.

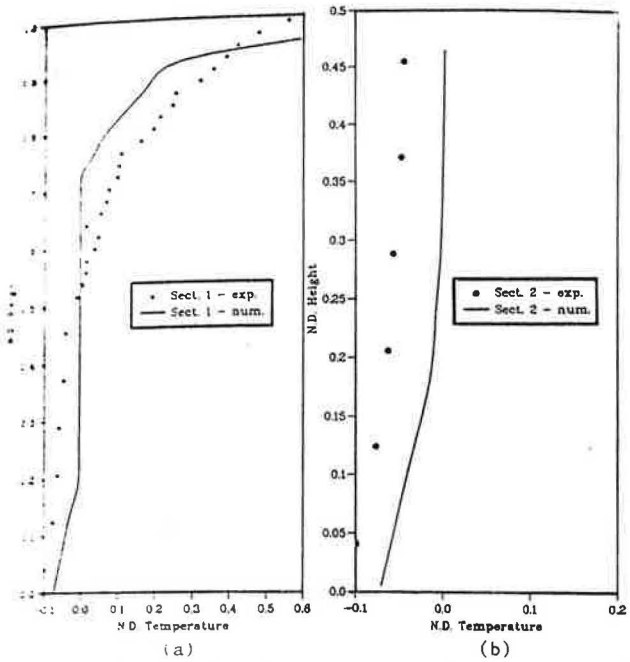

Figure 8. Predicted and measured temperature profiles. (a) at section #1; (b) at section #2.

Figure 9 (a) and (b) reports for the under-roof region on predicted and measured temperature profiles at sections #3 and #4, respectively. In both cases the predictions agree well with the measurements, however, in section #4, in the upper region from 0.635 to 0.660 of the normalized height some marked departures are apparent. The predicted heat transfer rates are much higher than those measured, an observation, which may support the importance of conduction heat transfer along the roof material, and the eventual need for its incorporation into the model.

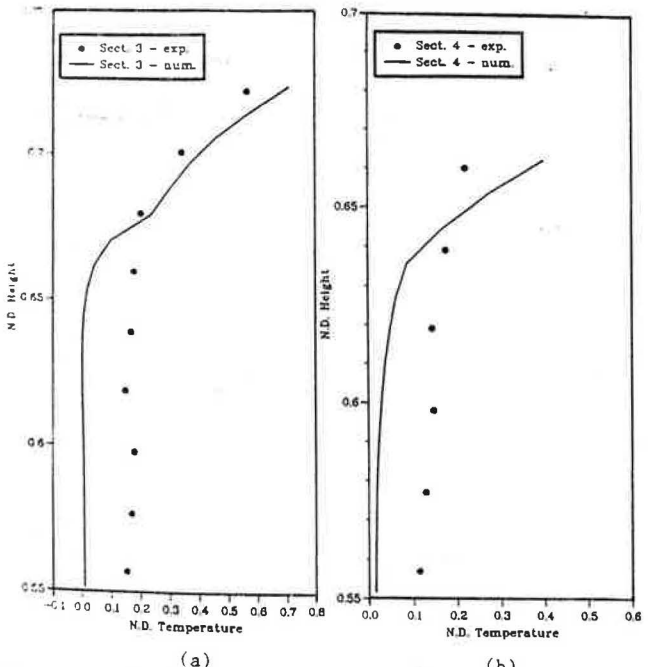

Figure 9. Predicted and measured temperature profiles: (a) at section #3; (b) at section #4.

CONCLUDING REMARKS

The primary findings of the present study allow the following conclusions.

The use of solar-driven ventilation applied to a bioclimatic building seems to be feasible. The preliminary results, however, indicate that the present design needs considerable modifications, since the cooling effect is very weak in the living space of the building. To improve and optimize the cooling performance new configurations for the chimney and windows, including registers and deflecting baffles, should be analysed through physical and numerical modelling, before a full-scale prototype can be built.

The predictions obtained via CFD, when compared against the experimental data, present a high level of reliability. The CFD model still requires further refinement, but even as it is, offers a very useful tool in evaluating and guiding future designs of the proposed concept of using a solar chimney to induce air flow. The present model captures well the main features of the velocity and temperature fields, despite their complexity.

ACKNOWLEDGEMENT

The ICTP Italian Labs Program supported M.S. Imbabi, while on sabbatical leave at Universita di Trieste. Natural Sciences and Engineering Research Council of Canada, through the International Collaborative Research Grant No. R0090041 facilitated the two-month stay of A.C.M. Sousa at University of Trieste. The computational work was performed at Computer Centre of the University of Trieste, and the Consiglio Nazionale delle Ricerche (Italy), CNR Grants No. 88.02502.07 and 87.01834.07, provided partial funding to the project.

NOMENCLATURE

a	coefficients of the discretized equations, Eq. 12, dimensionless
b	source term, Eq. 12, dimensionless
g	acceleration of gravity, m/s^2
Gr	Grashof number, Eq. 8, dimensionless
H	height of the experimental model, m
p	normalized pressure, dimensionless
P	pressure, N/m^2
Pr	Prandtl number, Eq. 6, dimensionless
Ra	Rayleigh number, Eq. 7, dimensionless
t	normalized temperature, dimensionless
T	temperature, K
T_0	ambient (reference) temperature, K
T_1	maximum measured temperature at the model's roof, K
u	normalized horizontal velocity component, dimensionless
U	horizontal velocity component, m/s
v	normalized vertical velocity component, dimensionless
V	vertical velocity component, m/s
x	normalized horizontal coordinate, dimensionless
X	horizontal coordinate, m
y	normalized vertical coordinate, dimensionless
Y	vertical coordinate, m

Greek Letters

α	thermal diffusivity, m^2/s
β	volumetric thermal expansion coefficient, 1/K
υ	kinematic viscosity, m^2/s
ρ	density, kg/m^3

ϕ general consured variable (= u, v or t), dimensionless

Subscripts

E, N, S, W node locations with reference to the nominal point P (East, North, South and West)

REFERENCES

Awbi, H.B. 1989. "Application of Computational Fluid Dynamics in Room Ventilation." *Building and Environment* 24: 115-127.

Barozzi, G.S., Imbabi, M.S., Nobile, E. and Sousa, A.C.M. 1991. "Small-scale and numerical modelling of a passive solar ventilation system." Submitted to *The 5th International Conference on Computational Methods and Experimental Measurements*, July 23-26, 1991, Montreal, Canada.

Ciofalo, M. and M.W. Collins. 1989. "Predictions of heat transfer for turbulent flow in plane and rib-roughened channels using large eddy simulation." Proceedings of the VII National Conference on Heat Transfer (Firenza, Italy, June 15-17, 1989). Societa Editrice Esculapio, Bologna, Italy, 57-71.

Clarke, J.A. 1987. "Building energy simulation: The state-of-the art." in *Workshop on interaction between physics and architecture in environmental conscious design*, International Centre for Theoretical Physics, Trieste (Italy).

Costa, R.; P. Piva; O. Barduzzi; I. Golubovic and M. Diaz. 1986. "Architettura Bioclimatica nell' area caldo-umida dei territori Yoruba (Nigeria)." Paper presented at *Energia e Ambiente Costruito - Tradizione e Innovazione*, Udine (Italy), 10-11th of October.

Davidson, L. 1989. "Ventilation by Displacement in a Three-Dimensional Room - A Numerical Study." *Building and Environment* 24: 363-372.

Imbabi, M.S. and W. Chiesa. 1990. "Procedimento per la riproduzione di edifici bioclimatici su modelli fisici in piccola scala." *Tecnica Italiana* 2: 187-199.

Markatos, N.C., M.R. Malin and G. Cox. 1982. "Mathematical Modelling of Buoyancy-induced Smoke Flow in Enclosures." *Int. J. Heat Mass Transfer* 25: 63-75.

Murakami, S. and S. Kato. 1989. "Numerical and Experimental Study on Room Airflow - 3-D Predictions using the k-e Turbulence Model." *Building and Environment* 24: 85-97.

Nielsen, P.V., A. Restivo and J.H. Whitelaw. 1979. "Buoyancy-affected flows in ventilated rooms." *Num. Heat Transfer* 2: 115-127.

Nobile, E., A.C.M. Sousa and G.S. Barozzi. 1989. "Turbulence modelling in confined natural convection." *Int. J. Heat and Technology* 7: 24-35.

Nobile, E., T. Russo and G.S. Barozzi. 1989. "An Efficient Parallel Algorithm for the Numerical Solution of Navier-Stokes Equations using Fortran Structured Multiprogramming." In *Supercomputers in Engineering: Fluid Flow and Stress Analysis Applications*, Eds. C.A. Brebbia and A. Peters, Computational Mechanics Publications, Southampton, U.K., 3-14.

Nobile, E., A.C.M. Sousa and G.S. Barozzi. 1990. "Turbulent buoyant flows in enclosures." in *Heat Transfer 90* 2, Ed. G. Hetsroni, Hemisphere Publ. Corp., Washington, D.C., 543-548.

Piva, P., 1989. "Bioclimatic Systems for Tropical Buildings." *Studies in Environmental Design in West Africa* 8: 101-110.

Schreuder, W.A. and J.P. Du Plessis. 1989. "Simulation of Air Flow About a Directly Air Cooled Heat Exchanger." *Building and Environment* 24: 23-32.

Theodossiou, V.M. and A.C.M. Sousa. 1986. "An efficient algorithm for solving the incompressible fluid flow equations." *Int. J. Num. Meth. Fluids* 6: 557-572.

Van Doormaal, J.P. and G.D. Raithby. 1984. "Enhancements of the SIMPLE method for predicting incompressible fluid flows." *Num. Heat Transfer* 7: 511-537.

ABOUT THE AUTHORS

G.S. Barozzi, Professor and Director, Istituto di Fisica Tecnica, Universita degli Studi di Trieste.
Research areas: Conjugate heat transfer, non-Newtonian flows, and exergy analysis of heat exchange devices.

M.S. Imbabi, Senior Lecturer, Department of Engineering, University of Aberdeen.
Research areas: Energy management in buildings, energy analysis and physical modelling of HVAC systems, and appropriate technologies.

E. Nobile, Sr. Research Associate, Istituto di Fisica Tecnica, Universita degli Studi di Trieste.
Research areas: CFD applied to laminar and turbulent free convection, supercomputing, and numerical and physical flow visualization.

A.C.M. Sousa, Professor and Director of Graduate Studies, Department of Mechanical Engineering, University of New Brunswick.
Research areas: Numerical and physical modelling of single- and two-phase convective systems, Darcy flows in anisotropic media, and turbulence modelling.